ISSN 1996-3343

Asian Journal of Applied Sciences

http://knowledgiascientific.com

Knowledgia SCIENTIFIC
A Place to Publish Outstanding Research

Asian Journal of Applied Sciences 4 (1): 30-41, 2011
ISSN 1996-3343 / DOI: 10.3923/ajaps.2011.30.41

Experimental and Computational Investigation of Effects of Cooling Intake Air in NO_x Reduction and Performance of Diesel Engines

[1]S.M. Lashkarpour, [2]K. Bahlouli, [1]S.E. Razavi and [1]S. Marami Milani

[1]Department of Mechanical Engineering, Tabriz University, Sardrood Road, I.T.M. Co. Complex, Motorsazan Co. R and D Center, P.O. Box 51845-337, Tabriz, Iran

[2]Department of Mechanical Engineering, Eastern Mediterranean University, Famagusta, Cyprus

Corresponding Author: S.M. Lashkarpour, Department of Mechanical Engineering, Tabriz University, Sardrood Road, I.T.M. Co. Complex, Motorsazan Co. R and D Center, P.O. Box 51845-337, Tabriz, Iran Tel: +989357956052 Fax: +98 411 4245945-6

ABSTRACT

This study through the experimental and numerical investigation shows how the intercooler reduces NO_x while making the engine performance improved and soot formation decreased. The effects of intercooler on combustion process will be investigated. Also numerical study was performed to investigate the global incylinder characteristics of intercooler system by means of FIRE-CFD code. Results indicated that although the rate of premixed burning increases by using of intercooler due to higher ignition delay period but as a result of lower temperatures in all combustion cycles the NO_x emission decreases. Cooling intake air was an effective technique to reduce NO_x emission and have shown a reduction of NO_x by more than 50% for some operating conditions.

Key words: Intercooler, emission, NO_x reduction, FIRE-CFD code, combustion

INTRODUCTION

The direct injection diesel engines continue to have excellent benefits in fuel consumption and durability over other engines. It is very appealing to reduce emissions within the combustion cycle, thus avoiding the necessity for exhaust after-treatment.

Research and development efforts are focused on NO_x reduction technologies. The NO_x is mainly produced due to high temperature. Therefore, NO_x reduction is generally achieved by reducing the maximum gas temperature. Reducing the ignition delay, reducing the air temperature, controlling the position where the heat is released and controlling the maximum and duration of heat release are currently being used for NO_x reduction (Patterson and Henein, 1972; Heywood, 1988). The common way to control NO_x has been using the turbocharging with intercooling and retarding the fuel injection. Retarding increases BSFC and deteriorates fuel economy (Challen and Baranescu, 1999). The most important engine parameters for NO_x reduction are: fuel injection timing, intercooling, inlet flow, combustion chamber design, fuel injection rate and compression ratio (Desantes *et al*., 2004a, b; Ikegami *et al*., 1997).

In particular, high pressure fuel injection turned out to be effective in decreasing smoke and PM considerably and thus has been considered as a key technique. Such injection method, however, aggravates NO_x and noise (Jorach and Doppler, 2000; Dohle *et al*., 2004). Further measures to reduce pollutants in engine raw emissions are intercooling, cooled and non-cooled

exhaust gas recirculation, water injection (especially ship engines) (Zheng *et al.*, 2004; Aabo and Kjiemtrup, 2004; Hulpi, 2004) and the early closing of the intake valves (Miller cycle). An increase of charge pressure (reduction of soot due to increased amount of oxygen) combined with reduced compression ratios (prevention of increased peak temperatures and NO_x -formation) is also advantageous (Mewes and Mayinger, 2006).

Experimental engine testing provides an invaluable means of investigating things such as the effect intake air has on engine performance. However, measurements inside the cylinder can be invasive and complicated to setup and are only able to ascertain some properties at a few discrete points in the cylinder. In response, Computational Fluid Dynamics (CFD) emerged as a companion to experimental work in engine design. While CFD should not be used to the exclusion of experimental data due to limitations in accuracy, it facilitates the visualization of all fluid parameters throughout a domain and allows for relatively easy modifications to the domain.

Consequently, the FIRE-CFD code was used in this work to model the effects of cooling intake air on combustion and emissions in the MT4.244 diesel engine. The ultimate goal is to gain a detailed understanding of cooling intake air properties and determining the effects of intercooling air on combustion and formation of pollutants.

MATERIALS AND METHODS

The engine under study is a commercial DI, water cooled four cylinders, in-line, turbocharged aspirated diesel engine whose major specifications are shown in Table 1.

The mass flow meter works on a hot wire anemometer principle. This well-established measurement method is based on a system whereby heat is extracted from a heated body by the gas flowing around it. Flow-dependent cooling is used as a measuring effect. It is possible to cover a very large measuring range with constant accuracy (max. error 1% of the measured value). With a high accuracy mass flow sensor, the fuel consumption is determined continuously via direct mass flow measurement in kg h^{-1}. Temperatures of cooling water, lubricating oil, inlet air and exhaust gases were also measured to ensure proper engine operating conditions. A data acquisition system was used to collect the important data and store them in a personal computer for exact analysis. Figure 1 shows Schematic diagram of experimental set-up.

Table 1: Engine specification

Engine specification	Description
Engine name	MT4.244
Bore (mm)	100
Stroke (mm)	127.0
Displacement (L)	3.99
Combustion chamber	Reentrant
Compression ratio	17.5
Number of valves/cylinder	2/4
Injection type	Direct
Fuel injection pump	DPA
Injection pressure (bar)	450-500
Fuel injection nozzle	5 hole
Maximum power output (kW)	61.5 kW at 2000 rpm
Maximum torque output (Nm)	340 Nm at 1400 rpm
Kind of aspiration	Turbocharged

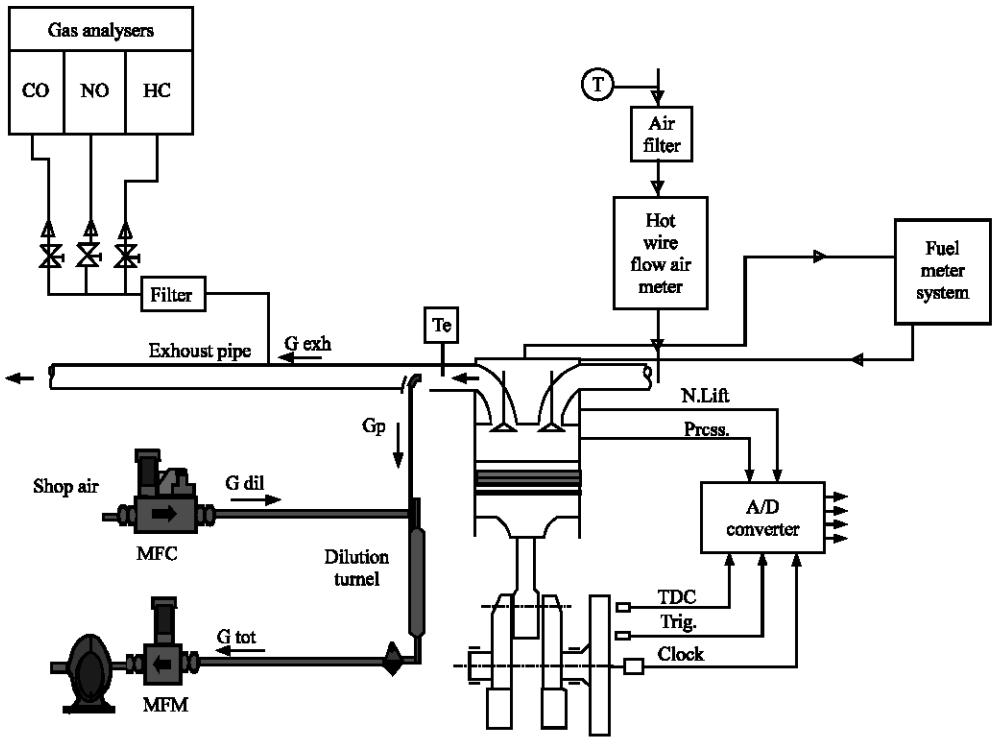

Fig. 1: Schematic diagram of experimental set-up

A piezoelectric type pressure transducer (Indi Modul 621) was flush-mounted with the combustion chamber for routine sampling of the cylinder pressure traces. Cylinder pressure was measured at every 0.1 crank angles. Engine crank shaft position was determined by a crank angle encoder. The fuel injector was instrumented with a hall-effect needle lift sensor which provided indications of the start and end of fuel injection events.

Particulate concentrations were determined by measuring filter weight before and after sampling (AVL SPC 472_Model CE 97). A separate probe was used for particulate matter sampling. The temperature of the probe was maintained above 190°C to prevent condensation. The exhaust sample was then diluted in a mini-dilution tunnel using filtered and dried air. The total mass flow rate of the tunnel (G_{tot}) and the mass flow rate of diluted air (G_{dil}) were measured and controlled by SPC. The mass flow rate of the exhaust flow was calculated as the difference of the other two flows. The heated probe was mounted after the mixing tank to sample the gaseous emissions in the exhaust.

Other engine emissions were measured using an AVL Dicom4000-class1 exhaust gas analyzer. Unburned hydrocarbons, CO and CO_2 were measured using a non dispersive infrared detector while an electrochemical detector was used for O_2 and NO_x measurements.

Experimental procedure: Experiments were conducted on a DI diesel engine connected with a D.C. magnetic dynamometer. Pollutant emission measurements were performed according to the (ECE-R96), 8 mode procedure as shown in Table 2. To ensure the measurement accuracy, all emission analyzers were calibrated before and after each test run. The emission measurements at each mode were repeated five times. The averaged values of repeated measurements were used in

Table 2: 8-mode procedure

Mode	Speed (rpm)	Load (%)	Condition No.	Weighting factor
1	2000	100	1	0.15
2	2000	75	-	0.15
3	2000	50	-	0.15
4	2000	25	-	0.10
5	1400	100	2	0.10
6	1400	50	-	0.10
7	1400	25	-	0.10
8	Idle	-	-	0.15

Table 3: Repeatability of measurements

Emissions	NO_x	PM	Fuel cons.
SD/Mean (%)	0.9	4.3	0.4

the analysis. From the repeated data points, the repeatability of the engine experiments can be estimated. The standard deviations over the means of the emission data are shown in Table 3. It can be seen from Table 3 that NO_x emission measurement repeatability is excellent, whereas all other measurements have good repeatability.

Combustion and emissions were monitored for engine base engine (condition 1-Full load with maximum power) and engine with intercooler (condition 2-Full load with maximum torque) to reduce emission level of engine and were compared with stage 3A standard. Condition 1 and 2 are mentioned at Table 2.

Computational modeling: In the context of transient IC engine simulations, FIRE has already been recognized of being the leading CFD solution in terms of three dimensional simulations of fluid flow, mixture formation, combustion and pollutant formation in direct injection diesel engine. With the open software architecture and well defined model interfaces, FIRE serves as a generic CFD platform for easy integration of all kinds of alternative spray, mixture formation and combustion/pollutant formation models.

Additionally, the CFD code FIRE also provides its own broad range of validated spray, combustion and pollutant formation models. A CFD FIRE code was used to simulate the overall combustion processes of the MT4.244 stageII diesel engine. The complete computational methodology applied in this study includes three-step hierarchy: (1) geometry and grid generation, (2) boundary conditions, (3) discretization scheme.

The Three-dimensional geometry is first modeled in SolidWorks software in full aspects including intake and exhaust ports, intake and exhaust valves and cylinder. Notice that the intake port is tangential and the bowl is reentrant and non symmetric. The geometry data are output in a parasolid file format. The surface grid generation is done by importing the geometry data into the ICEM CFD code. The ICEM CFD code is used to generate a surface mesh as STL file format which acceptable as a surface mesh by FIRE. So the geometry is known by means of STL surface mesh. The hybrid mesher which included in FIRE is then used to generate the volume mesh with interval size 0.002, which consisted of hexahedral dominated meshes. The exhaust port calculations in the present study are ignored due to simplification.

Figure 2a and b show the computational model with final volume mesh. Number of cells in the mesh was about 177.669 at TDC. This fine mesh size with specified number will be able to provide independent results as good as appropriate spatial resolution for the distribution of most variable within the computational domain.

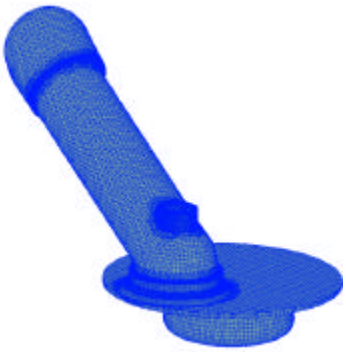

Fig. 2: Computational mesh for inlet port and combustion chamber at TDC

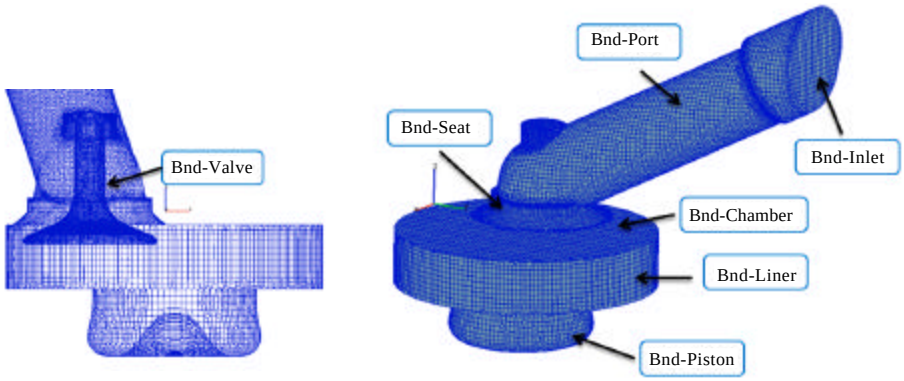

Fig. 3: Grid configurations and boundary conditions at 40 ATDC

Boundary conditions: Figure 3 shows the boundary conditions that used in computational domain at 40 ATDC. In this work Bnd refers to boundary condition.

Intake pressure has been measured within induction period of working processes with relative pressure sensor and used as boundary condition at Bnd-inlet. For determining the start of injection and injection duration, needle lift sensor has used as indicated in Fig. 4. The initial and boundary conditions of the engine are shown in Table 4.

Model elements: A stochastic dispersion model was employed to take the effect of interaction between the particles and the turbulent eddies into account by adding a fluctuating velocity to the mean gas velocity (Gosman and Ioannides, 1981). This model assumes that the fluctuating velocity has a randomly Gaussian distribution. The spray-wall interaction model used in the simulations is based on the spray-wall impingement model described by Naber and Reitz (1988). This model assumes that a droplet, which hits the wall is affected by rebound or reflection based on the Weber number. The Dukowicz (1979) model was applied for treating the heat-up and evaporation of the droplet. This model assumes a uniform droplet temperature. In addition, the rate of droplet temperature change is determined by the heat balance, which states that the heat convection from the gas to the droplet either heats up the droplet or supplies heat for vaporization.

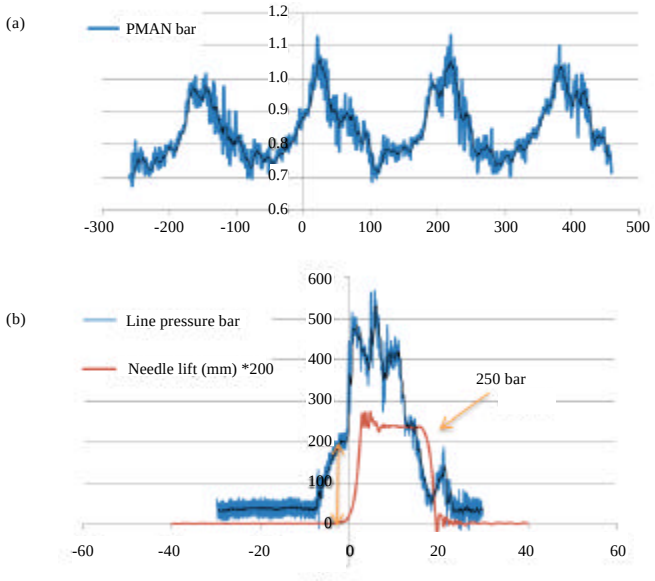

Fig. 4: (a) Inlet boundary condition Needle lift and (b) injection pressure curves

Table 4: Boundary and initial conditions of the engine

Boundary conditions	Type of BC
Bnd-Inlet	Inlet- P form Fig. 4-T = 400K
Bnd-Port	Wall-T = 400K
Bnd-Seat	Wall-T = 400K
Bnd-Valve	Wall-Mesh Movement- T = 400K
Bnd-Chamber	Wall-T = 500K
Bnd-Liner	Wall-T = 450K
Bnd-Piston	Wall-Mesh Movement-T = 450K
Initial conditions	**Values**
Engine speed	2000 rpm
TKE	8 m^2 sec^{-2}
TLS	0.01 m
Initial chamber pressure	126 kpa
Initial chamber temperature	430 K
Initial port pressure	120 kpa
Initial port temperature	370 K

The Shell auto-ignition model was used for modeling of the auto-ignition (Halstead *et al*., 1977). In this generic mechanism, six generic species for hydrocarbon fuel, oxidizer, total radical pool, branching agent, intermediate species and products were involved. In addition the important stages of auto-ignition such as initiation, propagation, branching and termination were presented by generalized reactions, described by Halstead *et al*. (1977), but this not mean that we used just 6 spices for reaction mechanism. The Eddy Breakup Model (EBU) based on the turbulent mixing was used for modeling of the combustion in the bowl (Magnussen and Hjertager, 1977). This model assumes that chemistry occurs fast and the combustion is mixing-controlled. The Zeldovich mechanism (Lavoie *et al*., 1970) was used for prediction of No_x

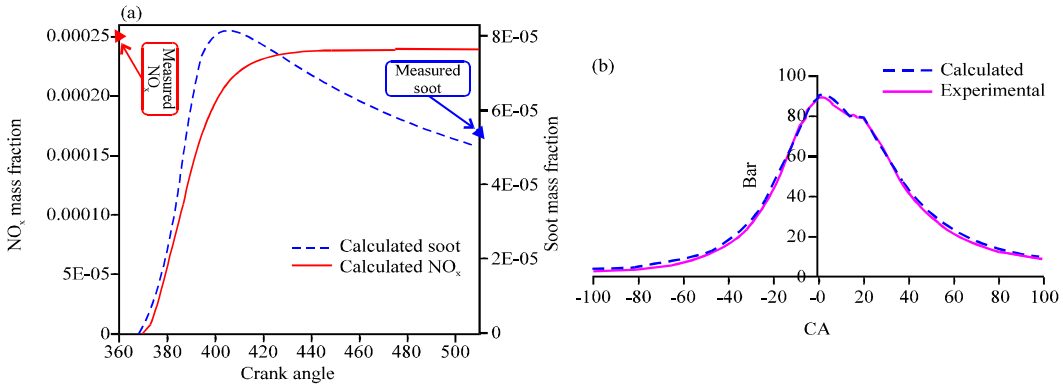

Fig. 5: (a, b) Pressure vs. crank angle NO_x and Soot traces with respect to crank angle l. for computed and experimental case for condition 1

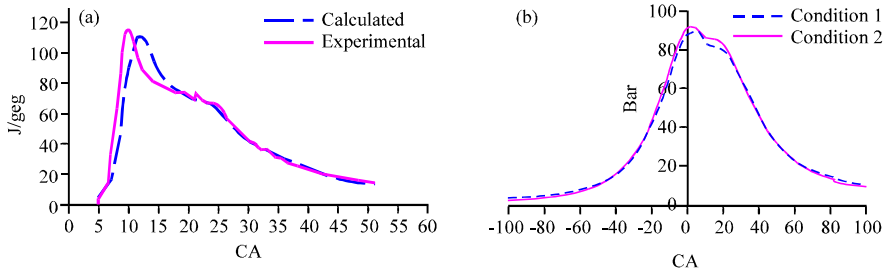

Fig. 6: (a, b) Pressure and Heat release Histories for engine in condition 1 and 2 at mode 1

formation. The trend for soot was determined in a different way, i.e., by mapping the equivalence ratio and temperature over all computational cells as described by Kaario *et al*. (2005).

Model validation: Figure 5a and b show the pressure and the soot and NO_x histories with respect to crank angle with the base engine. As can be seen in Fig. 5 pressure traces show good agreement with the experimental data. And the engine-out NO_x and soot values match the experimental values well.

RESULTS AND DISCUSSION

Figure 6a and b show the engine cylinder pressure and heat release rate histories with crank position for condition 1 and 2, at 1st mode of 8-mode standard test procedure, respectively. The major change in heat release history due to using intercooler occurred in early stage of combustion (i.e., mostly in the period known as premixed burning). Although with cooling intake air, the magnitude of heat release rate peak associated with the premixed burning increases to small extent. But lower cylinder charge temperatures (Fig. 7) and lower premixed period led to lower NO_x emissions (Fig. 8).

It should be noted that a simple comparison of the mixing controlled burning period is not sufficient to explain observed emission trends. It may be expected that PM emission increases for this condition because of lower combustion temperature resulting in lower soot oxidation rate and thus higher PM level but it is also possible that intake air cooling causes to increase the inlet air density resulting high local air/fuel ratios and consequently leads to lower PM emission.

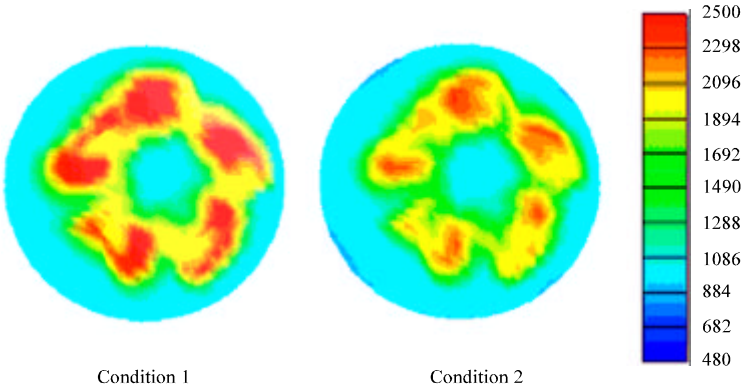

Fig. 7: Temperature evolution for engine in condition 1 and 2 at 40ATDC for mode 1

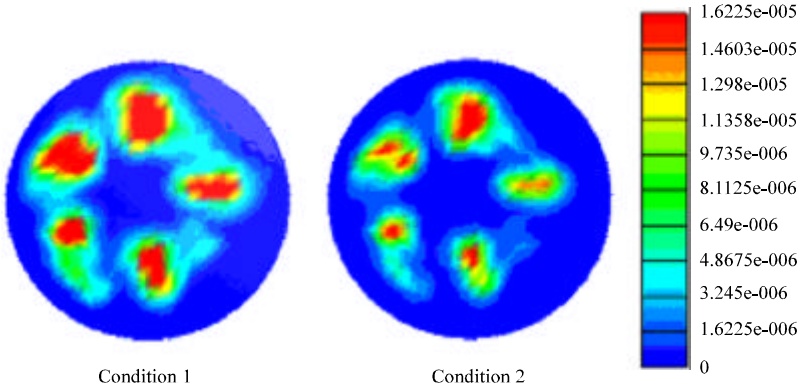

Fig. 8: NO_x Histories for engine in condition 1 and 2 at 40ATDC for mode 1

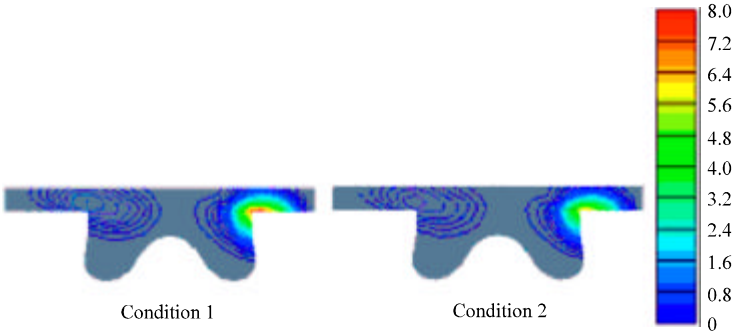

Fig. 9: Combustion Fuel/air ratio histories for engine in condition 1 and 2 at mode 1

Figure 9 shows combustion fuel/air ratio at 40ATDC for condition 1 and condition 2. It can be seen that the amount of fuel/air ratio decreases in the case of intercooler due to higher air introducing to engine cylinder. Intercooling also reduced thermal stresses to wall. Cooling the intake air leads to higher air densities and reduced spray penetration as shown in Fig. 10a and b.

Figure 11 and 12 show variation of the brake torque and bsfc versus engine speed at condition 1 and 2, respectively. It can be seen that both of these performance parameters improve by using intercooler due to introducing higher amount of air to the engine cylinders.

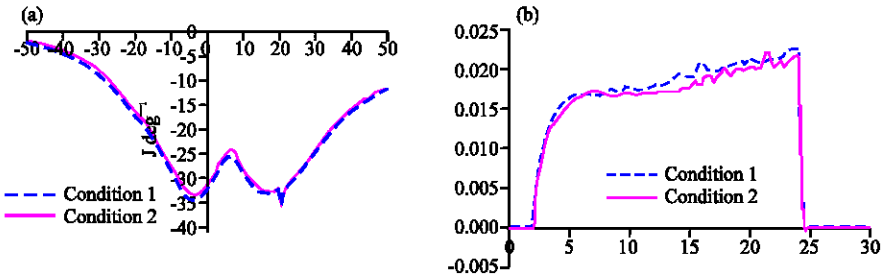

Fig. 10: (a, b) Heat flux to wall and jet penetration

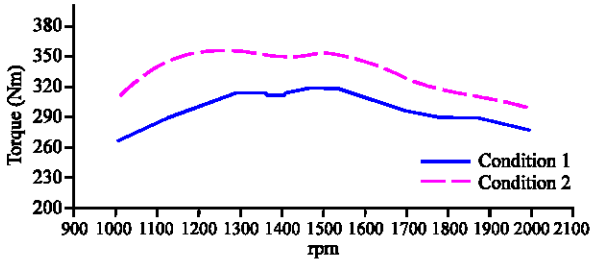

Fig. 11: Comparison of engine torque in condition 1 and 2

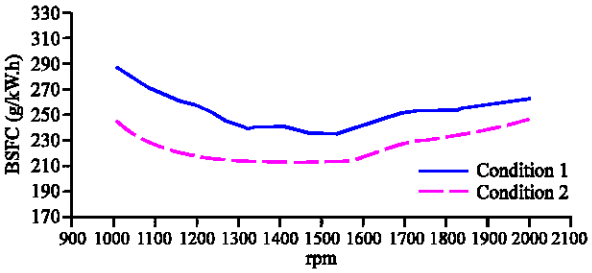

Fig. 12: Comparison of engine bsfc in condition 1 and 2

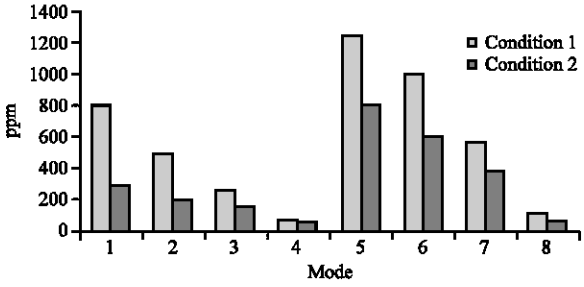

Fig. 13: Engine NO_x emissions for different modes of test procedure (conditions 1 and 2)

Figure 13 shows the amount of NO_x emission for all of the 8 mode s of the standard test procedure at condition 1 and 2. As indicated in this Fig. 13, NO_x emission decreases in all modes. This reduction is due to the lower amounts of cylinder charge temperature at condition 2 in comparison to condition 1.

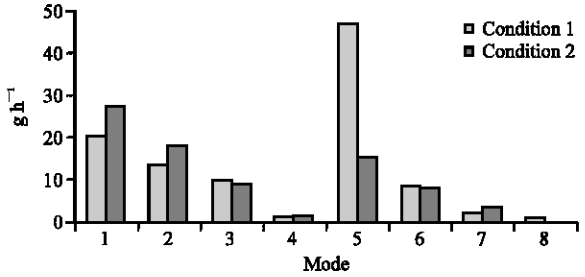

Fig. 14: Engine PM Emissions for different modes of test procedure (conditions 1 and 2)

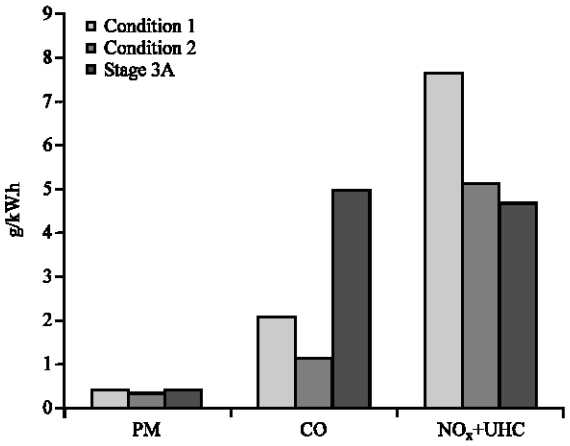

Fig. 15: Comparison of engine 8-mode (ECE-R96), test results in condition 1 and 2

As indicated in Fig. 14, almost in low speed modes, specially at mode 5, PM decreases as a result of higher air fuel ratio and it improves the soot oxidation. But at high speed modes specially at mode 1 and 2, PM increases.

Intercooling shows two different effects on soot formation. There are a variety of concurrent conditions contributing to this behavior. The main factor that affects soot is the cylinder charge density increase due to cooling of intake air which can increase the local oxygen availability. The other important factor is that higher air densities can reduce spray penetration leading to less expanded spray plumes resulting in reduced locally proper air fuel distribution and on the other hand they may also prevent spray impingement on the piston and cylinder walls. In general, at mode 5 and mode 6 (low speed modes) the dominant factor seems to be higher air fuel ratio which can enhance the oxidation through elevated oxygen partial pressures. Therefore, the test results show that PM emission decreases in these modes. But at mode 1 and mode 2 (high speed modes) the other factors are dominant which yield to increase in PM emission.

Figure 15 shows the comparison of PM, CO and NO_x+UHC between condition 1 and 2 and stage 3A standard level. It can be seen that all of emissions decrease by using intercooler.

CONCLUSIONS

Effects of intercooler on combustion process were investigated. Also Computational Fluid Dynamics (CFD) emerged as a companion to experimental work in engine design. The main results can be summarized as below:

- Intake charge cooling in a turbocharged engine can improve performance and emission characteristics
- Intake charge cooling can increase the local oxygen availability and also affect spray penetration and spray impingement and so it has different effects on PM emission
- Intake charge cooling reduced jet penetration due to increasing incylinder charge density
- Intake charge cooling reduced heat flux resulting lower thermal stresses

ACKNOWLEDGMENT

This work was supported by R & D Department of Motorsazan Company. Special thanks to Dr. R. Khoshbakhti Saray Assistant Professor of Sahand University of Technology, Tabriz, Iran for his useful guides.

REFERENCES

Aabo, K. and N. Kjiemtrup, 2004. Latest on emission control water emulsion and exhaust gas Re-circulation. Proceedings of the 2004 CIMAC Conference, Kyoto, Paper 126.

Challen, B. and R. Baranescu, 1999. Diesel Engine Reference Book. 2nd Edn., Butterworth, Heinemann, Oxford, ISBN-10: 0768004039.

Desantes, J.M., J. Benajes, S. Molina and C.A. Gonzalez, 2004a. The modification of the fuel injection rate in heavy-duty diesel engines. Part 1: Effects on engine performance and emissions. Applied Thermal Eng., 24: 2701-2714.

Desantes, J.M., J. Benajes, S. Molina and C.A. Gonzalez, 2004b. The modification of the fuel injection rate in heavy-duty diesel engines. Part 2: Effects on combustion. Applied Thermal Eng., 24: 2715-2726.

Dohle, U., M. Dürnholz, S. Kampmann, J. Hammer and C. Hinrichsen, 2004. 4th generation diesel common-rail injection system for future emission legislation. Proceedings of the FISITA World Automotive Congress, Barcelona, Paper F2004V271.

Dukowicz, J.K., 1979. Quasi-steady droplet change in the presence of convection, informal report Los Alamos Scientific Laboratory. LA7997-MS. http://searchworks.stanford.edu/view/2575550.

Gosman, A.D. and E. Ioannides, 1981. Aspects of computer simulation of liquid-fueled combustors. Proceedings of the 91th American Institute of Aeronautics and Astronautics, Aerospace Sciences Meeting, Jan. 12-15, St. Louis, Mo., pp: 11-11.

Halstead, M.P., L. Kirsch and C. Quinn, 1977. The auto-ignition of hydrocarbon fueled at high temperatures and pressures-fitting of a mathematical model. Combust Flame, 30: 45-60.

Heywood, J.B., 1988. Internal Combustion Engine Fundamentals. 1st Edn. McGraw-Hill, New York, ISBN: 0-07-028637-X.

Hulpi, J., 2004. Humidification methods for reduction of NO_x emissions. CIMAC Congress 2004, Kyoto, Paper No. 112.

Ikegami, M., K. Nakatani, S. Tanaka and K. Yamane, 1997. Fuel injection rate shaping and its effect on exhaust emissions in a direct-injection diesel engine using a spool acceleration type injection system. SAE Trans., 106: 524-535.

Jorach, R.W. and H. Doppler, 2000. Altmann: Heavy fuel common rail injection systems for large engines. MTZ Worldwide, 61: 10-13.

Kaario, O., E. Antila and M. Larmi, 2005. Applying soot Phi-T maps for engineering CFD applications in diesel engines. SAE 2005-01-3856, 2005. http://www.sae.org/technical/papers/2005-01-3856.

Lavoie, G.A., J.B. Heywood and J.C. Keck, 1970. Experimental and theoretical study of nitric oxide formation in internal combustion engines. Combust. Sci. Technol., 1: 313-326.

Magnussen, B.F. and B.H. Hjertager, 1977. On mathematical modeling of turbulent combustion with special emphasis on soot formation and combustion. Symp. (Int.) Combust., 16: 719-729.

Mewes, D. and F. Mayinger, 2006. Heat and Mass Transfer. Springer-Verlag, New York, Heidelberg, ISBN: 13978-3-540-30835-5.

Naber, J.D. and R.D. Reitz, 1988. Modeling engine spray/wall impingement. SAE 880107. https://www.sae.org/technical/papers/880107.

Patterson, D.J. and N.A. Henein, 1972. Emissions From Combustion Engines and their Control. Arbor Science Publication Inc., Michigan, USA, ISBN: 0250975149.

Zheng, M., G.T. Reader and G.J. Hawley, 2004. Diesel engine exhaust gas recirculation-a review on advanced and novel concepts. J. Energy Convers. Manage., 45: 883-900.